

Adsorption of Brilliant Blue R on Biotic Precursor Based Carbon

FAZALULLAH KHAN-BANGASH AND SHAH ALAM
*Institute of Chemical Sciences, University of Peshawar,
Peshawar, 21250, Pakistan.*

(Received 20th March, 2006, revised 28th September, 2006)

Summary: Carbon prepared from the wood of *Ailanthus altissima*, activated at 400 °C and 800 °C was used to adsorb brilliant blue R from aqueous solution at 10 °C and 45 °C. Characterization of the activated carbon by XRD, SEM, EDS and FTIR show that the surfaces contain functional groups like carboxyl's and ketones which disappeared at 800 °C and favor the exposure of porous structural surfaces which enhance the adsorption capacity. Relatively high amount of carbon with respect to oxygen was found with the increase in activation temperature. First order, Bangham, Elovich, parabolic diffusion and power function equations were found to fit the kinetic adsorption data. The reaction rate increased with the increase in temperatures of adsorption/ activation. Thermodynamic parameters like ΔE^{\ddagger} , ΔH^{\ddagger} , ΔS^{\ddagger} and ΔG^{\ddagger} were calculated. The negative values of ΔS^{\ddagger} reflect the decrease in the disorder of the system at the solid-solution interface, during adsorption. Gibbs free energy (ΔG^{\ddagger}), represent the driving force for the affinity of dye for the carbon and it increased with the increase in adsorption/ activation temperature. The positive value of ΔH^{\ddagger} shows the endothermic of adsorption and decreases with the increase in adsorption/activation temperature. Batch studies showed that isotherm equations of Langmuir and Dubinin-Radushkevich are applied to the data.

Introduction

Biotic precursors such as coconut shells, palm-kernel shells, wood chips, sawdust, corn cobs, seeds etc. when carbonized at high temperature, yield porous carbonaceous product. Various methods are available for activation process but the most widely used are the treatment with heat at 400 - 1000 °C under conditions that permit the removal of nearly all the hydrocarbon contents. Chemical activation proceeds under conditions that prevent the deposition of hydrocarbons on the surface. Other methods of activation such as mixing with potassium hydroxide and solutions of nitric acid or a mixture of nitric and hydrochloric acid, also increases the porosity. The final carbonaceous product has several important uses for pollutant removal from domestic and industrial water supplies [1, 2]. More than 10,000 chemically different dyes are being manufactured, and the world dyestuff and dye intermediates production is estimated to be around 7×10^5 kg per annum [3]. These are mainly consumed in textiles, tanneries, pharmaceuticals, packed food industries, pulp and paper, paint and electroplating industries. The effluents from dye manufacturing and dye application processes are highly colored. Color in the receiving water bodies such as river or lakes can inhibit photosynthesis and its compounds can react with metal ions to form substances toxic to fish and other aquatic life [4]. Technologies presently

employed for color removal are based on the physicochemical processes such as dilution, adsorption, coagulation and flocculation, chemical precipitation, oxidation, ion-exchange, reverse osmosis and ultra filtration [5]. Adsorption is the most commonly used method. Activated carbon is the most popular adsorbent for the removal of soluble pollutants from wastewater [6, 7].

In the present study, activated carbon from the wood of *Ailanthus altissima* was prepared and characterized with the objective to evaluate its adsorption potential for the removal (kinetics and equilibrium) of dye from aqueous solution using a cheap precursor.

Results and Discussion

Characterization

Surface area of the Raw carbon, 400 °C and 800 °C activated carbon was $134 \text{ m}^2 \cdot \text{g}^{-1}$, $245 \text{ m}^2 \cdot \text{g}^{-1}$ and $260 \text{ m}^2 \cdot \text{g}^{-1}$ respectively. The increase in the surface area with rise in temperature is due to the driving off of the tar in the gaseous form that is trapped in the porous structure [8]. FTIR spectral bands of samples (Fig. 1-3) in the region of 2779.2 cm^{-1} , 2854.5 cm^{-1} and 2588.3 cm^{-1} is present only in Raw and 400 °C sample but absent in 800 °C and is

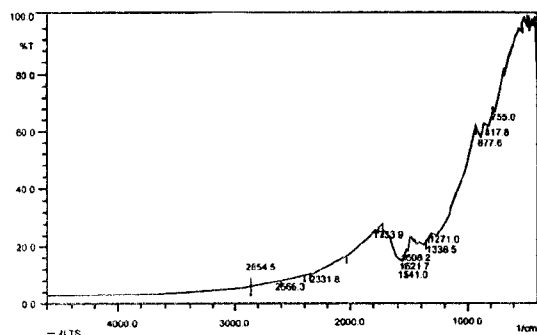


Fig. 1: FTIR spectra of Raw carbon sample.

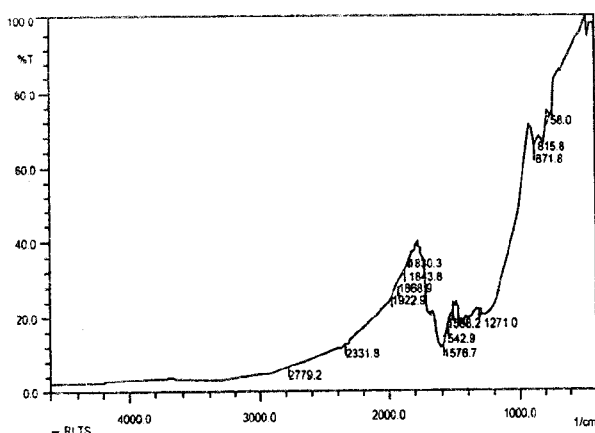


Fig. 2: FTIR spectra of 400 °C activated carbon sample.

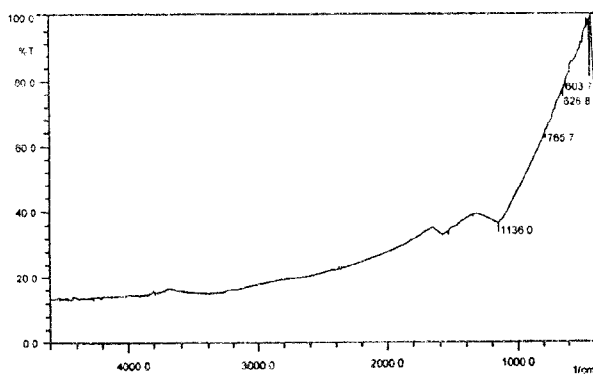


Fig. 3: FTIR spectra of 800 °C activated carbon sample.

ascribed to aliphatic $-CH_3$, $-CH_2$ and $-CH$ stretching. Peak at 2300 cm^{-1} is due to the presence of ketones [9]. A weak absorption bands in Raw and 400 °C at 1719 cm^{-1} represent $C=O$ stretching indicating the presence of various oxygen groups such as carboxyls [10]. The bands in the region $1000 - 1100\text{ cm}^{-1}$ confirm the presence of minerals matters [11], and between $900 - 700\text{ cm}^{-1}$ are aromatic bands for substituted benzene rings [9]. Scanning electron micrographs of the carbon samples before and after adsorption (Fig. 4 and 5) shows hexagonal shape pores and the surface being covered by the dye after adsorption. The energy dispersive spectra (Fig. 6 - 8) show that with the increase in activation temperature the carbon contents of the sample increases and oxygen is decreased (Table-1). The high oxygen contents on the surface of Raw sample and 400 °C activated carbon confirm the presence of oxygen surface functional groups which disappeared at high temperature, thus validating the FTIR analysis (Fig. 1-3). The X-ray diffraction patterns (Fig. 9 - 11) of carbon samples have a peak corresponding to $2\theta \approx 22^\circ$ which shows the disordered graphitic 002 planes

Table 1: Analysis (EDS) of carbon samples.

Samples	Elements	Weight %	Atomic %
Raw	C	77.73	83.48
	O	20.33	16.18
	Mg	0.200	0.100
	K	0.410	0.130
	Ca	0.330	0.110
400 °C	C	89.92	86.89
	O	15.33	12.21
	Cl	0.240	0.090
	K	2.210	0.720
	Fe	0.300	0.090
800 °C	C	86.97	91.57
	O	9.010	7.130
	Mg	0.170	0.090
	Cl	0.420	0.150
	K	2.810	0.910
	Ca	0.300	0.090
	Cu	0.320	0.060

Table-2: Some characteristics of carbon sample.

Physical Parameters	Raw	Activated carbon	
		400 °C	800 °C
pH	8.950	8.850	9.990
Ash Contents (%)	6.30	5.020	3.000
Bulk Density (kg/m^3)	210	195	165
Moisture content (%)	1.50	0.660	0.4200

Table-3: Elovich equation constants for the kinetics adsorption of brilliant blue R on carbon sample.

Samples	$(1/\beta)$		β	$(1/\beta) \ln(\infty\beta)$	σ	R^2
	10 °C	45 °C				
Raw	0.2167	1.023	4.6147	0.99772	0.1348	0.4511
400 °C	0.5607	0.8251	1.7835	1.21197	0.4282	0.3572
800 °C	0.6288	0.8326	1.59033	1.2011	0.6744	0.5810

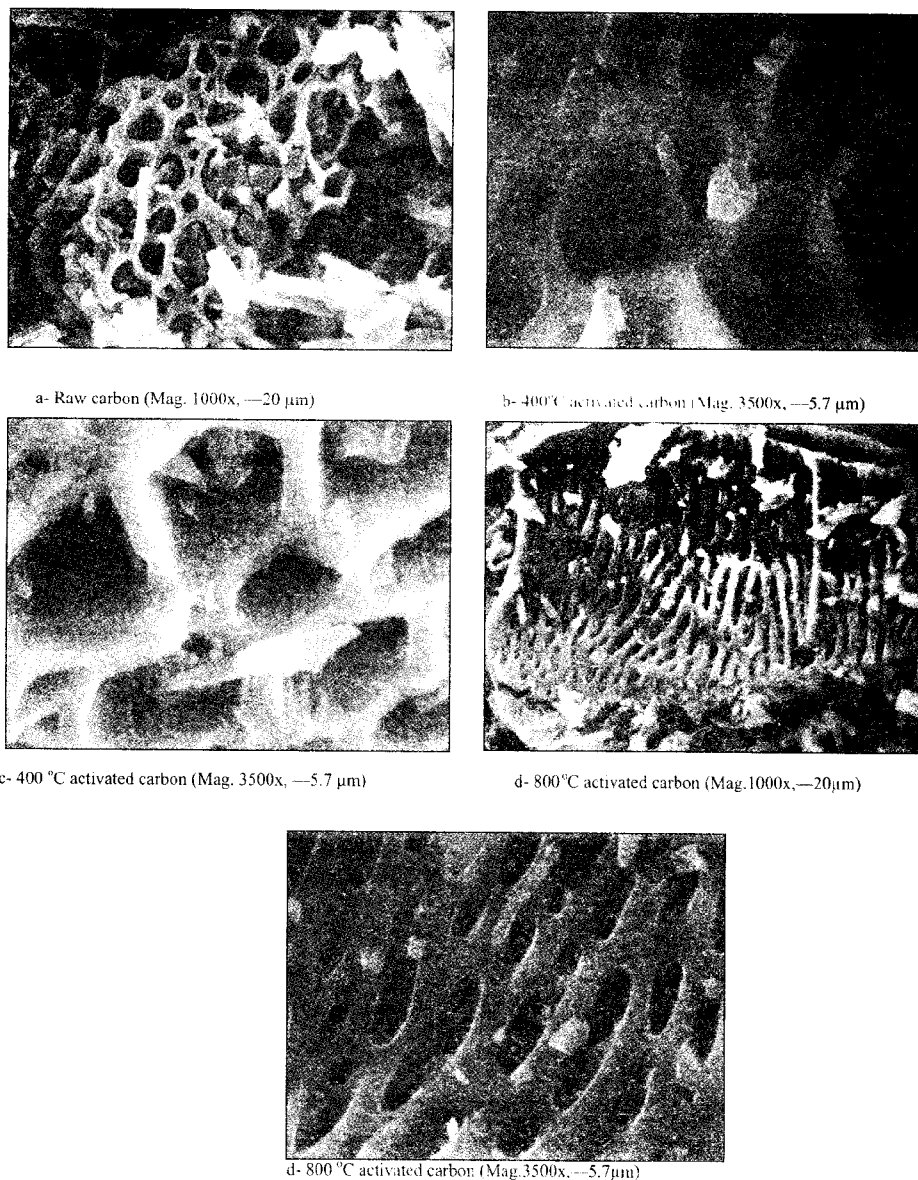


Fig. 4 (a - d): Scanning electron micrographs of carbon sample. (AccV =20kV, Signal = SEI, WD = 16mm, Spot Size = 25).

Table-4: Bangham equation constants for the adsorption kinetics of brilliant blue R on carbon sample.

Samples	∞		k_0		R^2	
	10°C	45°C	10°C	45°C	10°C	45°C
Raw	1.2322	0.8043	1.5474	5.8678	0.9392	0.9600
400 °C	0.2452	0.2961	14.0931	14.454	0.9288	0.9609
800 °C	0.2044	0.2452	16.610	16.999	0.972	0.9686

[10]. The Raw carbon shows the presence of phase like molybdenum sulfide chloride- $\text{Mo}(\text{S}_2)_3\text{SCL}_4$ [file number 74-2043], that of 400 °C show the presence of phase of chromium carbonyl cobalt tungsten phosphide- $(\text{CO})_5\text{Cr}(\text{CO})_5\text{WP}_2\text{CO}_2(\text{CO})_6$ [file number 77-2229]. The 800 °C degassed carbon shows the phase of 2, 4-dinitromesitylene- $\text{C}_9\text{H}_7\text{N}_2\text{O}_4$ [file number 13-0780].



(Mag = 1100x, AccV = 20kV, Signal = SEI, WD = 18mm, Spot Size = 26, -1.82 μm)

Fig. 5: Scanning electron micrographs (SEM) of carbon sample after adsorption.

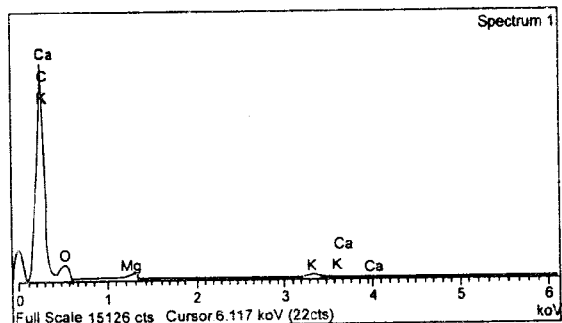


Fig. 6: Energy dispersive spectrum (EDS) of Raw carbon sample.

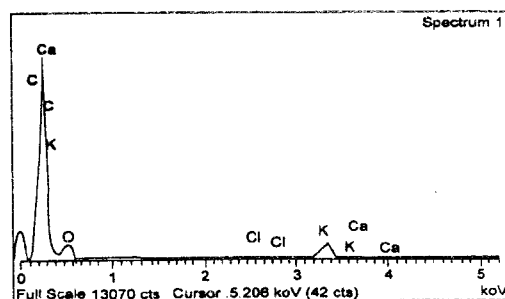


Fig. 7: Energy dispersive spectrum (EDS) of 400 °C activated carbon sample.

Adsorption Studies

The rate of adsorption of dye at 10 °C and 45 °C is high in the initial fifteen seconds and then it becomes slow due to the possible diffusion in to the micropores. The slow process continues and reaches to equilibrium in two hour time giving a plateau (Fig. 12 and 13). Linear forms of the kinetic equations (Table-10) were applied to the data and their goodness of fit was evaluated from correlation coefficient (R^2), standard error estimate (SE), variance ratio (F) and the level of significance of F statistic (P), (Table-9). Based on these parameters, it appears that adsorption kinetics of the dye on different carbon samples (Raw, degassed at 400 and 800 °C) can be described reasonably well by all the models applied.

The rate constant, k_{ad} (s^{-1}), from the slope of the linear plots (Fig. 14) increase with both the

Table-5: Thermodynamic parameters for the adsorption of brilliant blue R on carbon sample.

Thermodynamic Parameters	Samples					
	Raw		400 °C		800 °C	
	10 °C	45 °C	10 °C	45 °C	10 °C	45 °C
ΔH^\ddagger (kJ. mol ⁻¹)	38.10524	35.461388	9.08244	8.791448	6.31494	6.023948
ΔS^\ddagger (J. mol ⁻¹ . K ⁻¹)	-160.7073	-169.0713	-252.320	-253.290	-259.360	-260.329
ΔG^\ddagger (kJ. mol ⁻¹)	2.125210	53.77375	71.41564	80.55501	73.40519	82.79064
K_{ad} (s ⁻¹)	0.00220	0.01460	0.00820	0.014000	0.01140	0.017100

Table-6: Freundlich constants for the adsorption of brilliant blue R on carbon sample.

Samples	l/n		n		K (mol. g ⁻¹ × 10 ⁻³)	
	10 °C	45 °C	10 °C	45 °C	10 °C	45 °C
Raw	0.7683	0.5047	1.301	1.981	0.233	3.429
400 °C	0.497	0.4794	2.012	2.085	3.928	4.227
800 °C	0.323	0.3331	3.095	3.102	11.608	20.69

Table-7: Langmuir's constants for the adsorption of brilliant blue R on activated carbon sample.

Samples	(l/d)		d (mol/g)		1/Kd		K ₁	
	10 °C	45 °C	10 °C	45 °C	10 °C	45 °C	10 °C	45 °C
Raw	32.204	22.528	0.031052	0.04439	12.065	7.8963	2.6692	2.8529
400 °C	22.871	18.564	0.043723	0.05387	5.9659	5.0066	3.7336	3.7077
800 °C	21.3959	16.9184	0.046738	0.05911	1.5399	1.3015	12.8943	12.9985

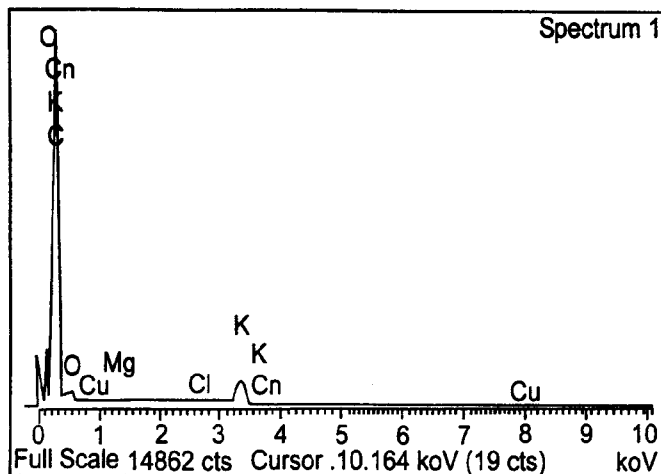


Fig. 8: Energy dispersive spectrum (EDS) of 800 °C activated carbon sample.

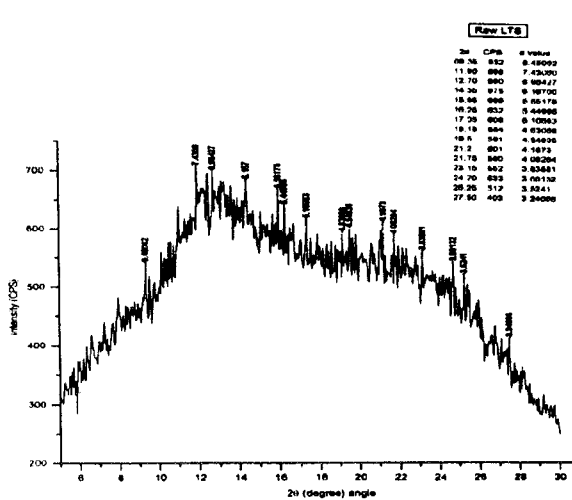


Fig. 9: XRD spectra of Raw carbon sample.

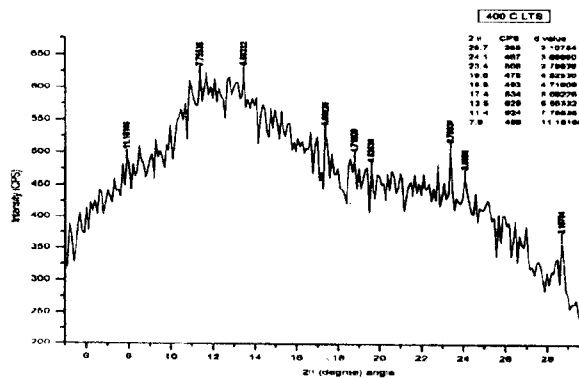


Fig. 10: XRD Spectra of 400 °C activated carbon sample.

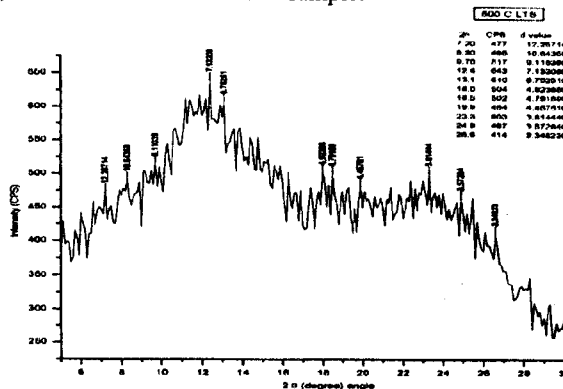


Fig. 11: XRD spectra of 800 °C activated carbon sample.

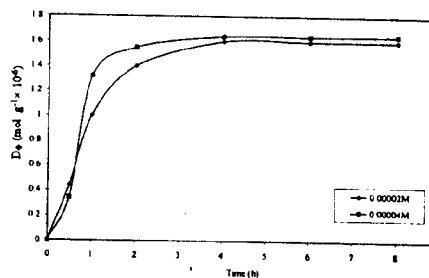


Fig. 12: Effect of contact time of brilliant blue R adsorption on carbon sample.

degassing and adsorption temperatures (Table 5). The energy of activation ($\text{kJ}\cdot\text{mol}^{-1}$) for the adsorption calculated from Arrhenius equation for Raw and carbon activated at 400 and 800 °C, are 40.4581, 11.4353 and 8.66780 respectively. From the activation

Table-8: Dubinin-Radushkevich equation constants for the adsorption of brilliant blue R on carbon sample.

Samples	$D_{\phi m}$		B		R^2	
	283K	318K	283K	318K	283K	318K
Raw	15.84168	56.38734	1.00632	1.0032	0.9193	0.8549
400 °C	63.576551	74.23566	1.00401	1.00290	0.9631	0.9194
800 °C	71.682362	75.056767	1.00260	1.00210	0.9453	0.8926

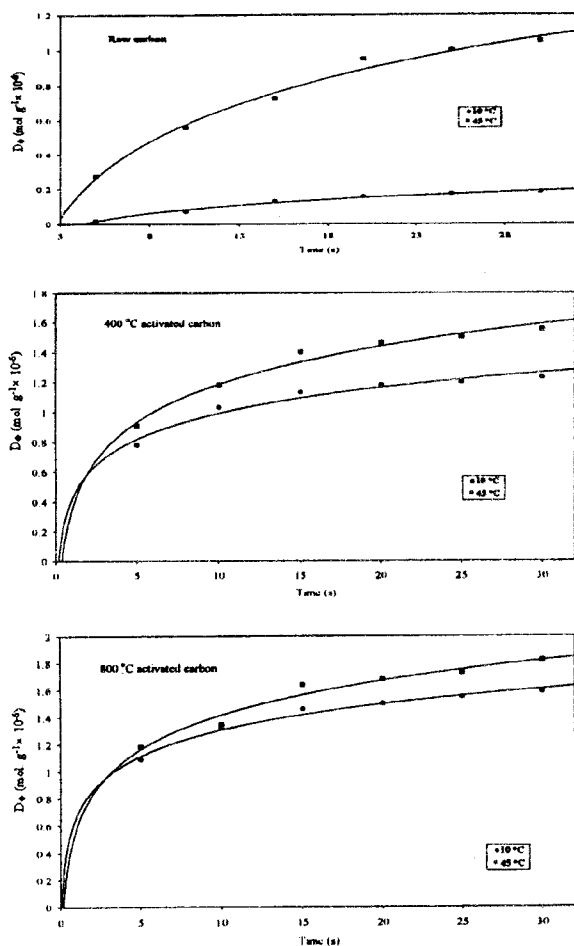


Fig. 13: Adsorption kinetics of brilliant blue R on carbon samples .

energy, values of enthalpy of activation (ΔH^\ddagger), entropy of activation (ΔS^\ddagger) and Gibb's free energy of activation (ΔG^\ddagger) were calculated [12]. The negative values of ΔS^\ddagger reflect the decrease in disorder of the system at the solid-solution interface during adsorption. Gibbs free energy (ΔG^\ddagger) represents the driving force [13] for the affinity of dye for the carbon and it increases with the increase in activation/adsorption. The positive value of ΔH^\ddagger shows the endothermic and spontaneous nature of

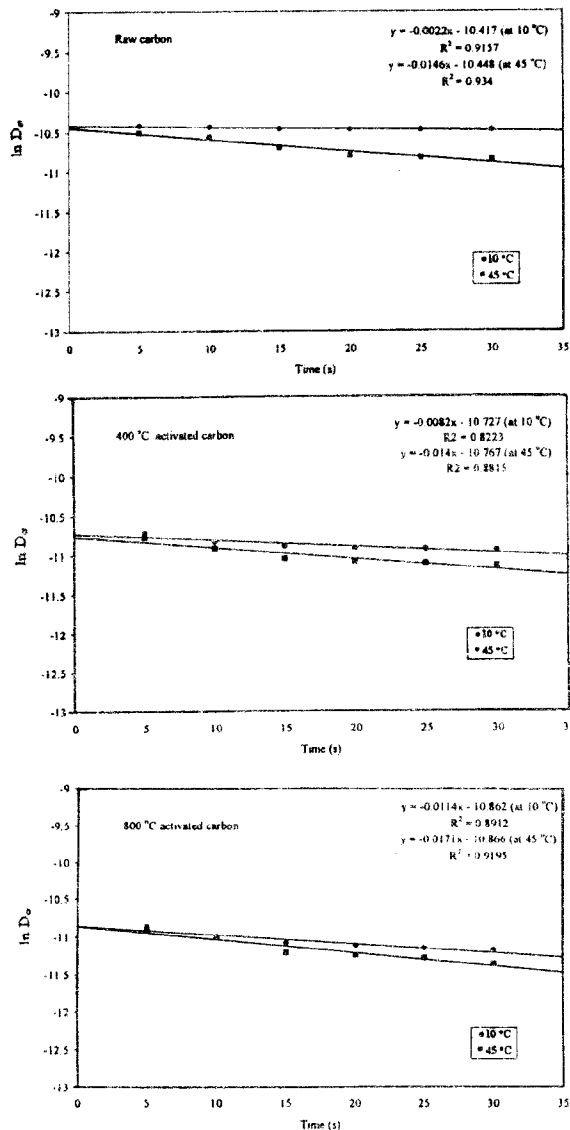


Fig. 14: First order kinetics plots of the brilliant blue R adsorption on carbon samples.

adsorption and decreases with the increase in adsorption/activation temperature (Table-5).

The α values obtained from the linear Bangham plots (Fig. 15, 16) indicate that the rate

Table 9: Mean values of SE, F statistics and P for different models fitted to kinetics adsorption of brilliant blue R on carbon sample.

Samples	Mean Values	Models									
		First Order		Elovich		Bangham		Power Function		Parabolic Function	
		10°C	45°C	10°C	45°C	10°C	45°C	10°C	45°C	10°C	45°C
Raw	SE ($\times 10^{-6}$)	0.0005592	0.0001184	0.000987	0.003164	0.000983	0.0005907	0.0007670	0.0007970	0.000576	0.000862
	F ($\times 10^{-4}$)	0.000097	0.000038	0.000710	0.000080	0.0008080	0.0005298	0.001623	0.000974	0.001220	0.000080
	P ($\times 10^{-4}$)	0.0000272	0.0000654	0.000760	0.003400	0.0001033	0.0002748	0.0009586	0.000645	0.000600	0.000400
400 °C	SE ($\times 10^{-6}$)	0.100074	0.007614	0.002294	0.007969	0.0005109	0.0009097	0.003530	0.000308	0.000290	0.001864
	F ($\times 10^{-4}$)	0.000088	0.000489	0.0004080	0.0006167	0.000200	0.0000610	0.008901	0.000059	0.000080	0.000700
	P ($\times 10^{-4}$)	0.0000731	0.0000078	0.000070	0.0000810	0.000833	0.0005509	0.008096	0.0034016	0.0010070	0.000805
800 °C	SE ($\times 10^{-6}$)	0.0007150	0.0004830	0.004535	0.006265	0.010121	0.003897	0.003700	0.000255	0.000247	0.0000625
	F ($\times 10^{-4}$)	0.0001700	0.0008100	0.006862	0.007569	0.0000646	0.000349	0.005055	0.000319	0.000602	0.0007569
	P ($\times 10^{-4}$)	0.0004779	0.006825	0.000720	0.0006307	0.0000539	0.000791	0.0000212	0.001009	0.0000720	0.0000307

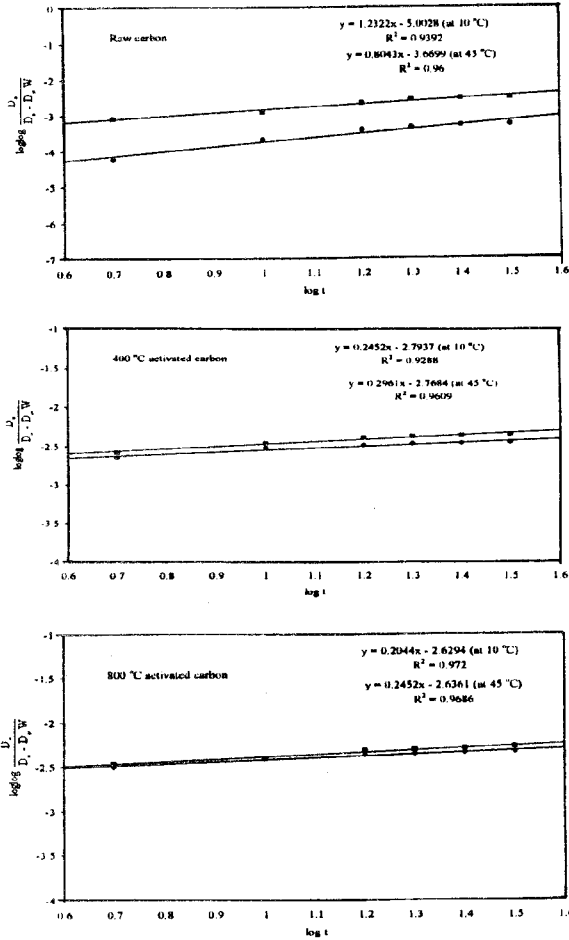


Fig. 15: Bangham plots of the brilliant blue R adsorption on carbon samples.

limiting steps in the uptake of dye is a diffusion controlled process [13]. The values of $\alpha < 1$ (Table-3), from the linear Elovich plots emphasize the site heterogeneity for the dye adsorption in the Raw and activated samples of 400 and 800 °C [14]. Parabolic diffusion law (Fig. 17) and power function (Fig. 18) give linear fit of the data which also conform to the

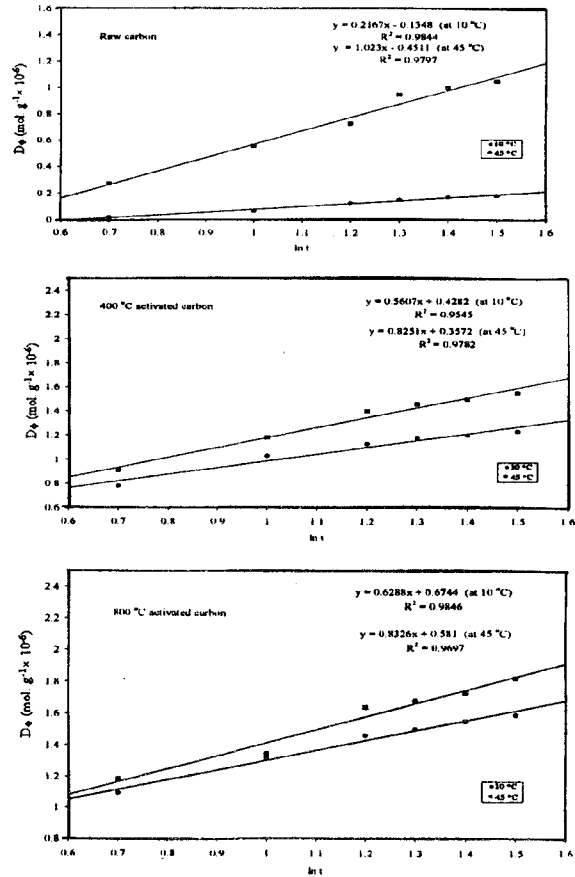


Fig. 16: Elovich plots of the brilliant blue R adsorption on carbon samples.

diffusion controlled process [15] for brilliant blue R adsorption on the activated carbon.

Batch Studies

Batch studies (Fig. 19) shows that the adsorption of dye on the samples is a function of activation temperature (Raw < 400 °C < 800 °C). Due to the presence of oxygen functional groups of carboxyls and ketones as indicated by FTIR spectra

Table 10: Different models that described the adsorption of brilliant blue R on carbon sample.

Model	Linear form
First order	$\ln D_{\sigma} = \ln D_0 - k_{ad} t$
Elovich	$D_{\sigma} = \left(\frac{1}{\beta}\right) \ln(\alpha\beta) + \frac{1}{\beta} \ln t$
Bangham	$\log \log \frac{D_0}{D_0 - D_{\sigma}} = \log \frac{k_{ad} W}{2.303 V} + \alpha \log t$
Power function	$\ln D_{\phi} = \ln(KQ_0) + 1/m \ln t$
Parabolic diffusion	$D_{\phi} = B + K_{ad} t^{1/2}$
Freundlich	$\ln D_{\phi} = \ln K + \frac{1}{n} \ln D_{\sigma}$
Langmuir	$\frac{D_{\sigma}}{D_{\phi}} = \frac{D_0}{d} + \frac{1}{Kd}$
Distribution coefficient	$D_{\sigma} = \frac{D_0 - D_{\phi}}{Wd}$
Dubinin-Radushkevich	$\ln D_{\phi} = \ln D_{\phi m} - B\epsilon^2$

Nomenclature

D_0	=	Initial concentration (mol.dm^{-3})
D_{ϕ}	=	Amount adsorbed (mol.g^{-1})
V	=	Volume of solution (dm^{-3})
W	=	Weight of carbon (g)
D_{σ}	=	Equilibrium concentration (mol.dm^{-3})
K_0 & α	=	Constants
ϵ	=	Polanyi potential
$D_{\phi m}$	=	Adsorption maximum
W_c	=	Weight of carbon
K	=	Rate constant
k_B	=	Boltzmann's constant ($1.3806 \times 10^{-23} \text{ J.K}^{-1}$)
h	=	Planck constant ($6.626 \times 10^{-34} \text{ J.s}$)
R	=	Universal gas constant ($8.314 \text{ J.K}^{-1}.\text{mol}^{-1}$)
SE	=	Standard error estimate
F	=	Variance ratio
P	=	Significance of F statistics

(Fig. 1 - 3) on the surface, the Raw and 400 °C samples have less adsorption. The applicability of the Freundlich equation [16] was found by the linear plots of $\ln D_{\phi}$ vs. $\ln D_{\sigma}$ (Fig. 20). The K values (Table 6) that measures the adsorption capacity, increases with the activation/ adsorption temperature. Application of Langmuir model [17] indicates monolayer coverage (Fig. 21) and the values of constant, K_1 increases with the adsorption/activation

temperature (Table-7). Dubinin-Radushkevich equation [18] gives linear plots of the adsorption data (Fig. 22) and the values of adsorption maximum ($D_{\phi m}$) found from the data, increased with the increase in activation temperature (Table-8).

The affinity of brilliant blue R determined from the distribution coefficients [19] for each point on the isotherms (Fig. 23), decreased as the adsorbate

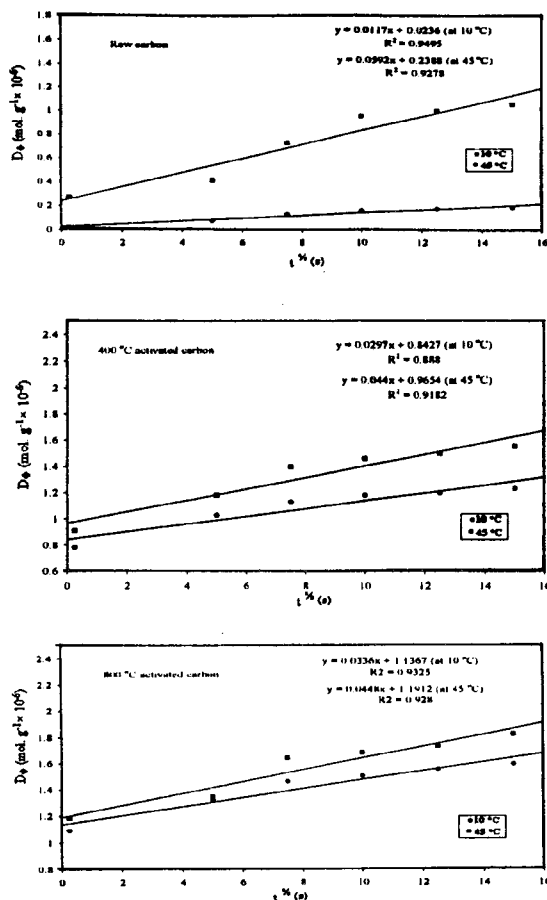


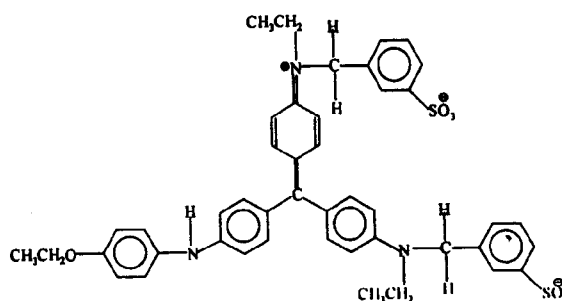
Fig. 17: Parabolic diffusion plots of the brilliant blue R adsorption on carbon samples.

concentration in the system increased over the range: $1 \times 10^{-5} - 5.5 \times 10^{-5}$ M. The values of distribution coefficient for the samples were found to be in the sequence $D_{f, Raw} < D_{f, 400 \text{ } ^\circ\text{C}} < D_{f, 800 \text{ } ^\circ\text{C}}$.

Experimental

Brilliant blue R

The dye used was supplied by Sigma-Aldrich (Catalogue No. = 37, 920 - 4 (178), dye contents = 50 %, formula weight = 825.99, λ_{max} = 588 nm) and has molecular structure,



Acid Blue 83 (Brilliant Blue R)

burner in a specially designed iron container with an outlet for the emission of volatile matter. Carbon obtained (about half of the mass of wood) was cooled in the container and ground with the help of pestle and mortar and screened with US standards mesh

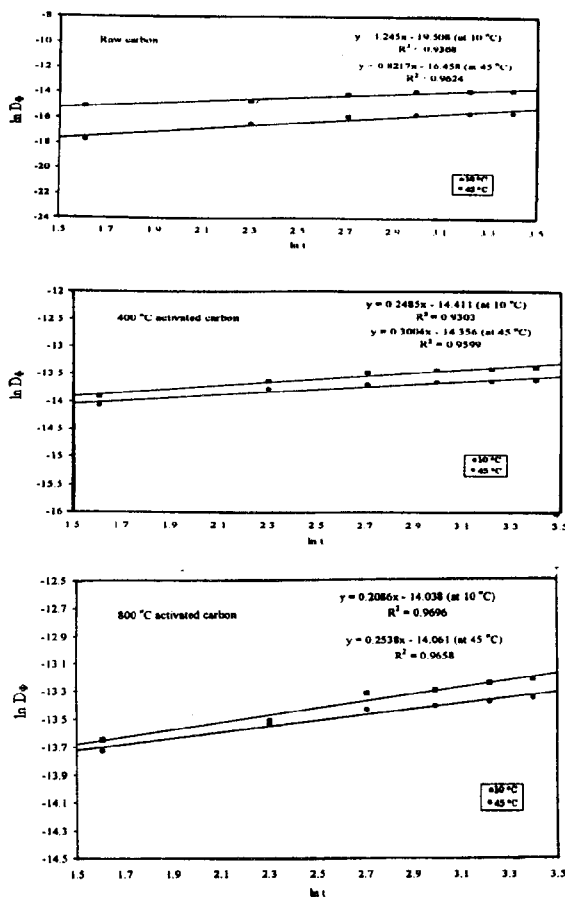


Fig. 18: Power function plots of the brilliant blue R adsorption on carbon samples.

Preparation of Carbon

The wood of *Ailanthus altissima* was air dried and then heated continuously for 5 hours on a flame

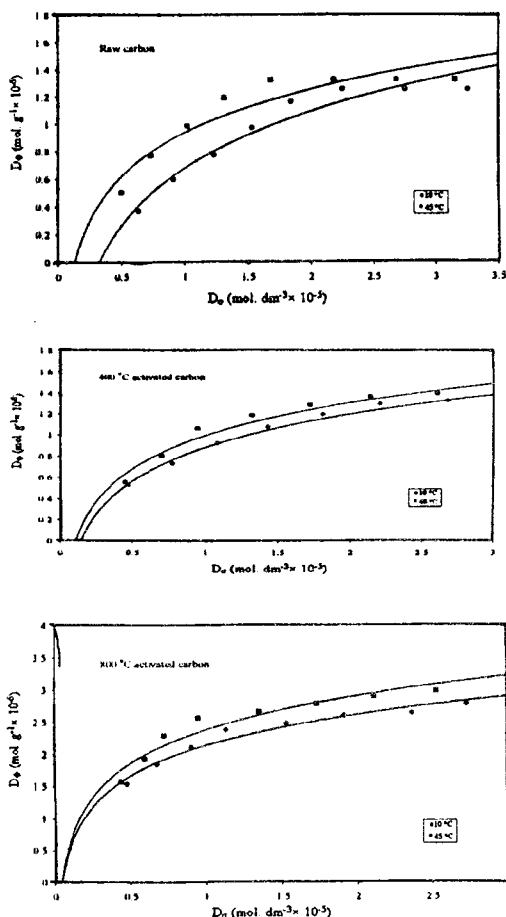


Fig. 19: Adsorption isotherm of brilliant blue R on carbon samples.

150-180 μm . It was then treated with 0.5 M aqueous solution of KOH for 24 hours with occasional stirring. The mixture was then filtered and washed with double distilled water for the complete removal of basicity. The carbon was then leached with 0.2N solution of HNO_3 : HCl (1: 1) and allowed to stand for 24 hours at room temperature with regular mixing. It was then filtered and washed with double distilled water until free from Cl^- and NO_3^- ions. The carbon thus obtained was then air-dried in an oven at 105 ± 1 °C. This treated carbon was then extracted with n-hexane for two hours in a soxhlet extractor and allowed to dry for 8 hours in a vacuum oven. The sample was then degassed by placing in silica (SiO_2) tubes, and heated at 400 and 800 °C in a tube furnace (FS. 215 Gallenkamp England), with a vacuum facility. The samples were allowed to cool and then stored under nitrogen atmosphere.

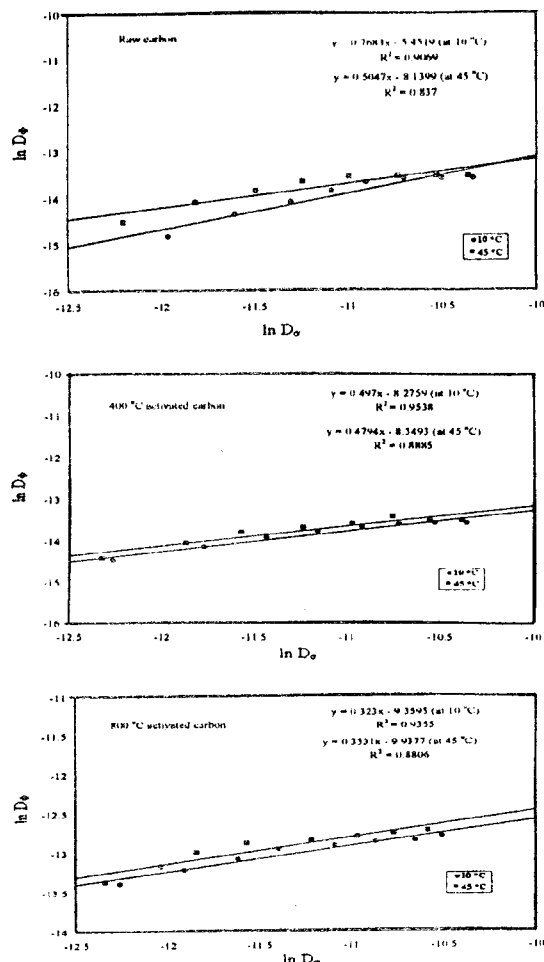


Fig. 20: Freundlich plots for the adsorption of brilliant blue R on carbon samples.

Characterization

pH of the prepared sample suspension in CO_2 free water (1: 50) was determined by pH meter. The moisture content was found by measuring the weight loss of the sample by heating for two hours at 105 ± 1 °C in an air dried oven. Ash content was obtained by ignition at 600 °C in a Muffle furnace, with door partially open to provide stream of air until the sample has been totally burned. The bulk density of the sample was also measured [20]. The surface area of the samples was determined as described elsewhere [21].

X-rays diffraction (XRD) analysis of the samples was done with X-rays diffractometer (RAD-1A, Rigaku Tokyo) using Cu $\text{K}\alpha$ radiation generated

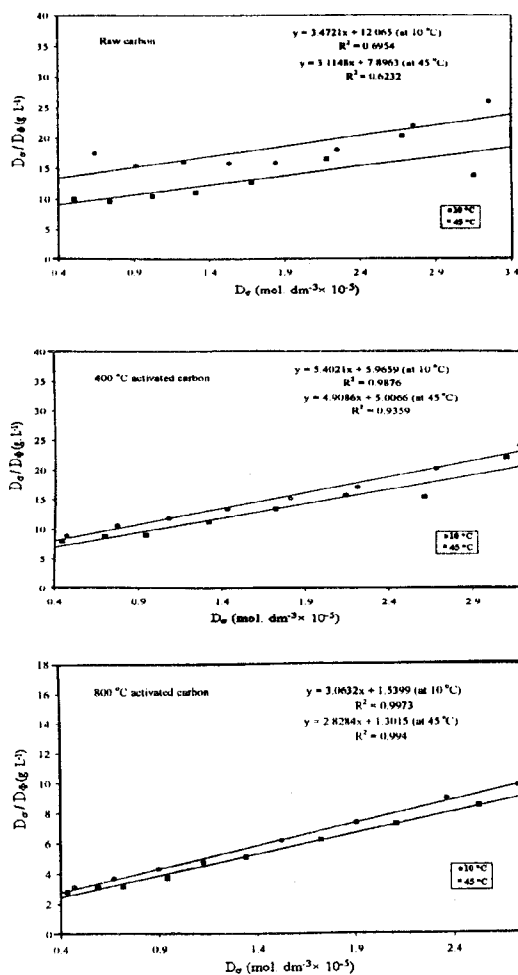


Fig. 21: Langmuir plots for the adsorption of brilliant blue R on carbon samples.

at 35 kV, 20 mA. The samples were filled in to the rectangular cavity of an aluminum sample holder and scanned in a step-scan mode (0.05° / step) over the angular range of 7 - 30° (2θ). FTIR spectral analysis of the KBr (Spectrosol BDH) mixed pallet of the sample was carried out by FTIR spectrometer (Shimadzu 8201PC with FTCOM-1 computer control disc unit). The surface morphology of the samples was studied by SEM (Model-JSM-5910, Japan JEOL) with EDS (INCA 200 Oxford Instruments) for the elemental analysis.

Effect of Contact Time

0.2 g of activated carbon and 20 cm³ of solution of brilliant blue R taken in a conical flask

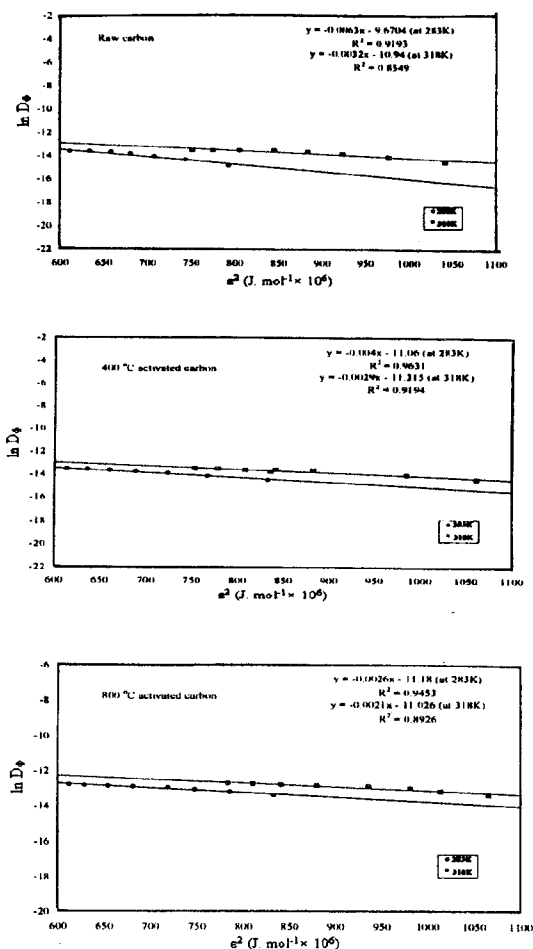


Fig. 22: Dubinin-Radushkevich plots for the adsorption of brilliant blue R on carbon samples.

was placed on a thermostated water bath shaker at 25 °C. A portion of the mixture was filtered after each time interval (0.5, 1, 2, 4, 6 and 8 hours). The concentration of the dye in the filtrate was determined by spectronic 20.

Adsorption Studies

For the adsorption kinetics, 0.2 g of activated carbon and 20cm³ of brilliant blue R (3.0 × 10⁻⁵ mol.dm⁻³) was shaken for different periods (5 - 30 seconds), in a laboratory syringe (Hamilton CO.) at 10 and 45 °C and filtered through 0.2 μ filter paper fitted in the syringe adopter. Batch experiments were also carried out at 10 and 45 °C by shaking 0.2 g of the sample with 20 cm³ of the dye solutions (1 × 10⁻⁵

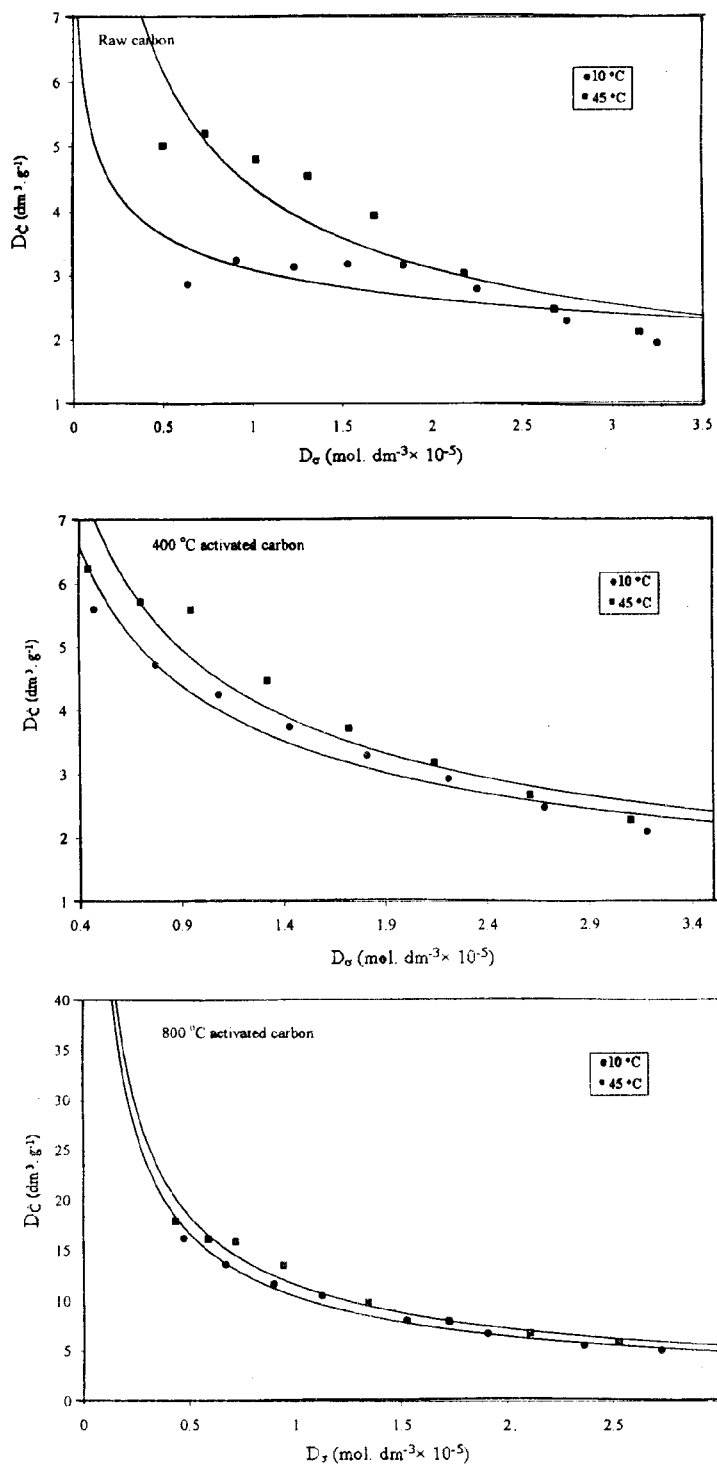


Fig. 23: Distribution coefficient plots for brilliant blue R in contact with carbon samples.

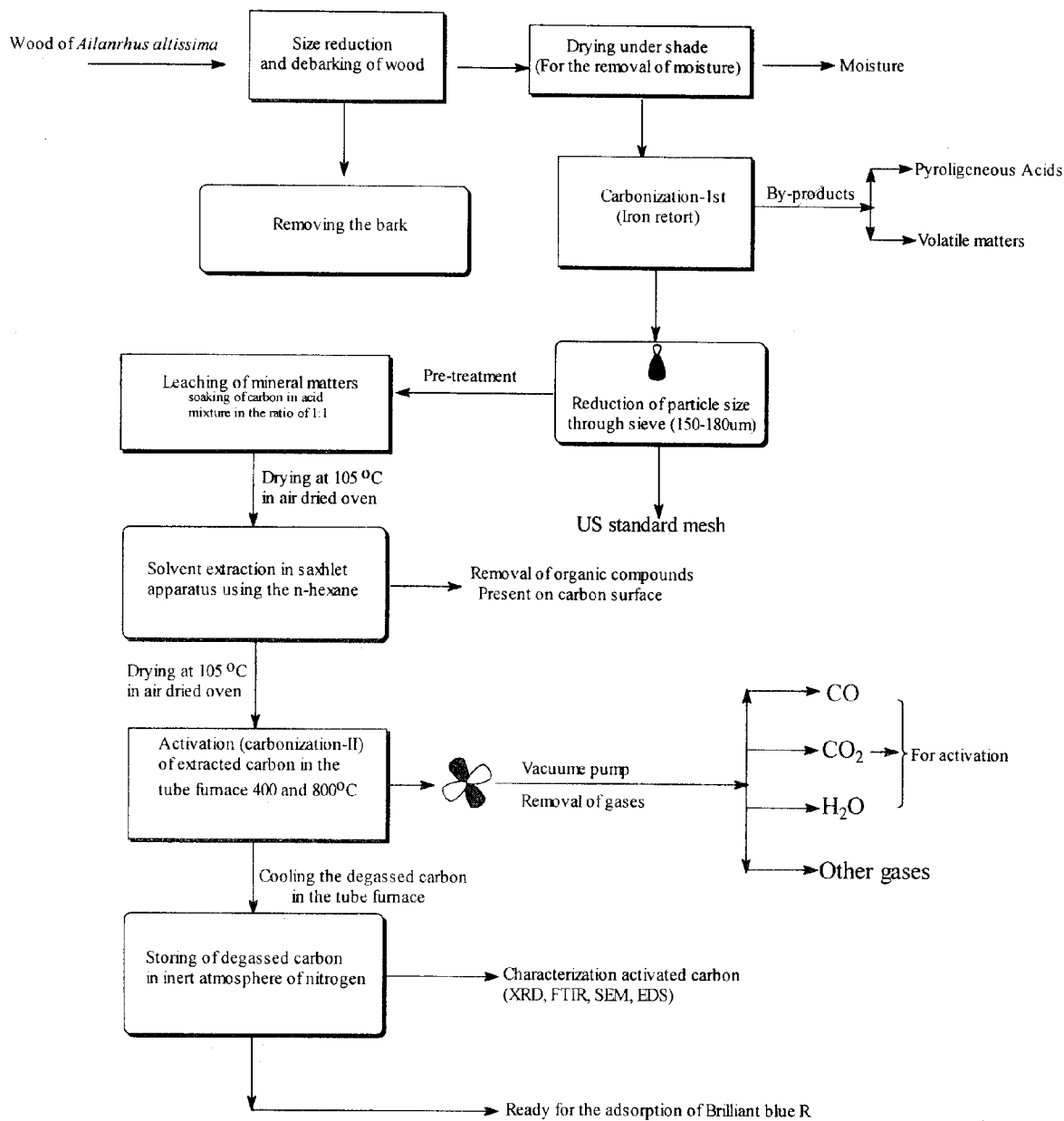


Fig. 24: Preparation of activated carbon from the wood of *Ailanthus altissima* (tree of heaven)

– 5.5×10^{-5} M) for two hours. The slurry was filtered and residual concentration of the dye in the filtrate was determined.

Conclusions

Activated carbon, prepared from *Ailanthus altissima* have surface functional groups like carboxyl's and ketones which disappear by activation at 800 °C thus improving the adsorption capacity. The EDS indicates increased relative amount of carbon w. r. t oxygen with the increase in activation temperature. First order, Bangham and Elovich equations were found to apply to the kinetic adsorption data. Langmuir and Dubinin-Radushkevich isotherms were also found to fit to the brilliant blue R adsorption, on the prepared carbon.

Acknowledgements

The authors thank the University of Peshawar for financial support. We thank Centralized Resource Laboratory (CRL), University of Peshawar, for providing research facilities.

References

1. F. K. Bangash, S. Alam, *Tenside Surf. Det.*, **43**(6), 299 (2006).
2. K. R. Ramakrishna and T. Viraraghavan, *Water Sci. Technol.*, **36**, 189 (1997).
3. A. A. Vaidya and K. V. Datye, *Colorate*, **14**, 3 (1982).
4. J. Karthikeyan, *Removal of Color from Industrial Effluents*. In: Trivedi, R. K. (Ed.), *Pollution Management in Industries*, Environmental Publication, Karad, India, 150 (1989).
5. I. Banat, P. Nigam, D. Singh and R. Marchant, *Bioresour. Technol.*, **58**, 217 (1996).
6. S. Babel and T. A. Kurniawan, *J. Hazardous Materials*, **97**, 219 (2003).
7. F. Derbyshire, M. Jagtoyen, R. Andrew, A. Rao, I. Martin-Gullon and E. Grulke, *Carbon Materials in Environmental Applications*. In: Radovic, L. R. (Ed.), *Chemistry and Physics of Carbon*, **27**, Marcel Dekker, New York, 1 (2001).
8. J. W. Hassler, *Purification with Activated Carbon*, Chemical Publishing CO. INC. New York, 176 (1974).
9. N. E. Cooke, O. M. Fuller and R. P. Gaikwad, *Fuel*, **65**, 1254 (1986).
10. K. Bhabendra, Pradhan and N. K. Sandle, *Carbon*, **32**, 123 (1999).
11. I. Ahmad, M. A. Khan, M. Ishaq, M. Shakirullah and A. Bahader, *J. Eng. and Appl. Sci.*, **23**, 117 (2004).
12. K. L. Laidler, *Chemical Kinetics*, McGraw-Hill, New York (1965).
13. R. Qadeer, J. Hanif, M. Saleem and M. Afzal, *Jour. Chem. Soc. Pak.*, **17**, 82 (1995).
14. P. Connor, J. B. Lewis and W. J. Thomas, *The Adsorption of Iodine by Graphite*. Proceedings of the Fifth Conference on Carbon-I, Pergamon Press, New York. 120 (1961).
15. D. L. Sparks, *Kinetics of Sorption/Release Reaction at the Soil Mineral/Water Interface*. In: Spark, D.L (Ed.), *Soil Physical Chemistry* 2nd ed. CRC Press, Boca Raton, FL (1999).
16. H. Z. Freundlich, *Phys. Chem. Soc.*, **57**, 385 (1966).
17. I. Langmuir, *J. Am. Chem. Soc.*, **40**, 1361 (1948).
18. M. M. Dubinin and L. V. Radushkevich, *Proc. Acad. Sci. USSR* **55** (1947).
19. L.B. Khalil, A. A. Amina and Th. El-Nabarawy, *Adsorp. Sci., Technol.*, **19**, 511 (2001).
20. D. F. Snell and C. L. Hilton, *Encyclopedia of Industrial Chemical Analysis*. Interscience Publishers, New York, 4, 431 (1967).
21. F. K. Bangash and A. Manaf, *Jour. Chem. Soc. Pak.*, **26**, 111 (2004).